Surface Geometric and Electronic Structures of $BaFe_2As_2(001)$

V. B. Nascimento,[1,*] Ang Li,[2] Dilushan R. Jayasundara,[2] Yi Xuan,[2] Jared O'Neal,[2] Shuheng Pan,[2] T. Y. Chien,[3] Biao Hu,[3] X. B. He,[1] Guorong Li,[3] A. S. Sefat,[4] M. A. McGuire,[4] B. C. Sales,[4] D. Mandrus,[4] M. H. Pan,[4] Jiandi Zhang,[1] R. Jin,[1] and E. W. Plummer[1]

[1]*Department of Physics and Astronomy, Louisiana State University, Baton Rouge, Louisiana 70803-4001, USA*
[2]*Department of Physics and Texas Center for Superconductivity, University of Houston, Houston, Texas 77204-5002, USA*
[3]*Department of Physics and Astronomy, The University of Tennessee, Knoxville, Tennessee 37996, USA*
[4]*Oak Ridge National Laboratory, Oak Ridge, Tennessee 37831, USA*

(Received 19 May 2009; published 14 August 2009)

$BaFe_2As_2$ exhibits properties that are characteristic of the parent compounds of the newly discovered iron (Fe)-based high-T_C superconductors. By combining real-space imaging of scanning tunneling microscopy and spectroscopy (STM + STS) with momentum-space quantitative low-energy electron diffraction (LEED), we have identified the surface plane of cleaved $BaFe_2As_2$ crystals as the As terminated Fe-As layer—the plane where superconductivity occurs. LEED and STM + STS data on the $BaFe_2As_2(001)$ surface indicate an ordered arsenic (As) terminated metallic surface without reconstruction or lattice distortion. It is surprising that STM images the different Fe-As orbitals associated with the orthorhombic structure, but not the As atoms in the surface plane.

DOI: 10.1103/PhysRevLett.103.076104 PACS numbers: 68.35.B−, 61.05.jd, 68.37.Ef, 73.20.−r

Recently discovered superconductivity in Fe-based compounds marked an important advance in endeavors to understand mechanisms for high transition temperature (T_C) superconductivity [1,2]. To date, four homologous series of Fe-based superconductors have been identified, which are commonly denoted as the 1111 phase (RFeAsO or RFePO with R = rare-earth-metal atom), 122 phase ($\mathcal{A}$FeAs with $\mathcal{A}$ = alkaline-earth-metal atom, or $(Sr_4Sc_2O_6)Fe_2P_2$ [3]), 111 phase (AFeAs with A − alkali-metal atom) and 11 phase (FeTe or FeSe). While superconductivity can be achieved either by chemical doping or by applying external pressure, the undoped parent compounds exhibit rich structural and physical properties. Of particular importance is that all the parent compounds undergo two successive phase transitions—a structural transition from a high-symmetry tetragonal to a low-symmetry orthorhombic phase, and a magnetic transition driven by antiferromagnetic (AFM) order [4–6]. Superconductivity occurs when both of these transitions are suppressed [7,8].

Among the four homologous series, the 122 system is unique. In this system superconductivity can occur without completely suppressing the AFM order—there is a noticeable region in the phase diagram where superconductivity and AFM coexist [9,10]. Thus, this is an ideal system for studying the interplay between superconductivity and magnetism. Single crystals of these new 122 materials, which form layered structures, can be easily cleaved to expose large flat surfaces. It is important both intellectually and technologically to address the physical properties of the surface of an ordered bulk material (single crystal), resulting from the effects of broken symmetry. Our experience with complex transition-metal oxides has shown that small structural distortions at the surface can have quite dramatic consequences on the physical and chemical properties [11,12]. A practical motivation for this work is related to the fact that several powerful experimental techniques, e.g., angle resolved photoemission spectroscopy (ARPES) and STM + STS, are by their very nature surface-sensitive techniques. Interpreting the experimental data requires a thorough understanding of the surface—both the structural and electronic properties. A recent review of STM results clearly illustrates a ''stripped'' reconstruction of the doped 122 compounds and surface reconstructed stripes in the parent compound $SrFe_2As_2$ [13].

In this Letter, we report results obtained from the (001) surface of $BaFe_2As_2$ single crystals using both STM + STS and LEED techniques. The $BaFe_2As_2$ compound forms a tetragonal structure with the $I4/mmm$ space group symmetry at high temperatures (T), consisting of alternatively stacking Ba and Fe-As layers [see Fig. 1(a)] [14,15]. The structural transition, from high-T tetragonal ($I4/mmm$) to low-T orthorhombic ($Fmmm$) symmetry, occurs near 140 K, with corresponding unit cells schematically presented in Figs. 1(a) and 1(b) [15]. Furthermore, a collinear AFM ordering sets in at about the same temperature, i.e., $T_N \sim 140$ K [15].

For the STM + STS measurements, $BaFe_2As_2$ single crystals [15] were first precooled to ~20 K in an UHV environment, then cleaved *in situ* to produce a clean (001) surface. After cleavage, it was immediately inserted into the STM head, which was already at the base temperature (~4.3 K). Subsequent STM + STS measurements were all performed at 4.3 K. For LEED measurements, $BaFe_2As_2$ single crystals were cleaved *in situ* under a base pressure of 2×10^{-9} Torr at room temperature, producing a mirror-like (001) surface. After cleavage, the sample was immediately introduced into the LEED chamber which was

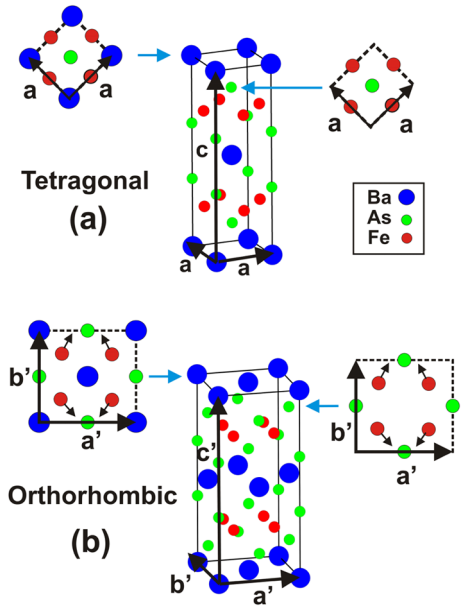

FIG. 1 (color online). (a) $BaFe_2As_2$ bulk unit cell for the high-temperature tetragonal phase. The (001) surface unit cells are shown for both Ba (left) and As terminations (right). (b) $BaFe_2As_2$ bulk unit cell for the low-temperature orthorhombic phase. The (001) surface unit cells are presented for Ba (left) and As terminations (right), where a' and b' lattice parameters are slightly different, i.e., 5.6146 and 5.5742 Å, respectively. The short black arrows indicate schematically the in-plane orthorhombic distortions of the Fe atoms when compared with the tetragonal phase. The Fe-Fe distances in the layer change from 2.8020 Å in the tetragonal phase, to 2.7870 and 2.8070 Å in the orthorhombic phase.

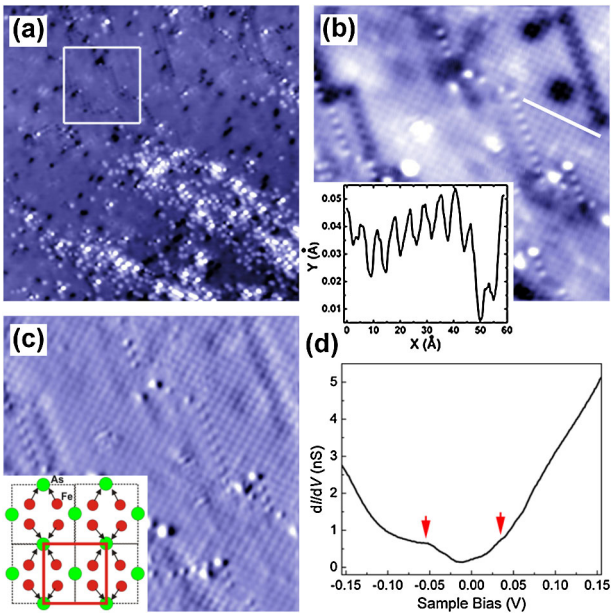

FIG. 2 (color online). (a) 800 × 800 Å constant-current topographic image ($V_{sample} = -100$ meV, $I_{tip} = 30$ pA) taken on a cleaved surface at 4.3 K. (b) 200 × 200 Å constant-current topographic image ($V_{sample} = -20$ meV, $I_{tip} = 8$ nA) zoomed into the area indicated by the white square box in (a). A line-profile along the white line in (b) is presented in the inset. (c) The current image obtained simultaneously with the image in (b). The inset schematically presents the two symmetrically distinct As atoms present in the orthorhombic surface unit cell, corresponding to the red square. (d) The representative tunneling spectrum taken on the surface in the areas far from those scattered atoms is presented.

maintained with a base pressure of 7.0×10^{-11} Torr, and cooled down to 20 K for experimental data collection.

Figure 2(a) shows an 800 × 800 Å topographic image of a cleaved $BaFe_2As_2$ surface taken at 4.3 K in constant-current mode. It reveals an atomically flat surface with many atoms (white dots) scattered, clustered, or piled on the surface without forming any ordered array. These atoms on the surface are relatively easy to move by the tip when the tip is very close to the surface. In addition to the atoms scattered on the surface, there are other features shown as dark spots and very weak chainlike structures in the atomically flat surface plane. Figure 2(b) is the constant-current topographic image when zooming into the area indicated by the white square box in Fig. 2(a). By pushing the tip closer to the surface (lowering the junction resistance), more details are revealed: (i) a "square"-like lattice with an in-plane lattice constant of ~5.6 Å appears clearly. Such a large lattice constant reflects a termination of primary $p(1 \times 1)$ structure truncated from an orthorhombic rather than a tetragonal bulk crystal (see Fig. 1); (ii) the larger white dots are the scattered Ba atoms without ordered structure; (iii) some dislocations or structural boundaries, shown as smaller white dots, form chainlike structures; and (iv) details of the darker spots and the zipperlike dark features are seen.

A line-profile of the image at the location indicated by the white line in Fig. 2(b) is presented as an inset, illustrating that the "squarelike" lattice corrugations are extremely small, with only 0.02 Å. It is worth emphasizing that the STM image reflects the morphology profile of the surface density of states (DOS) instead of the lattice of the atoms. For example, Fig. 1(b) shows that there are two environmentally distinct As atoms in each $p(1 \times 1)$ orthorhombic surface unit cell (5.6 × 5.6 Å), because of the motion of the Fe atoms in the second layer, but the STM image only shows one object per unit cell. The inset in Fig. 2(c) schematically presents the two distinct As atoms in the surface unit cell, one with four Fe ions slightly close to it and the other one with the Fe atoms slightly away from it, because of its orthorhombic distortion. STM measurements imply the existence of different Fe-As orbitals associated with the orthorhombic structure, because only the DOS of one type of As atoms was detected. By careful examination of the squarelike lattice, one can observe the small orthorhombicity distortion ($a' \neq b'$), usually expressed as $1 - b'/a'$. The orthorhombicity at the surface varies from 1% to 6% (depending on the location at the surface), larger that the 0.7% seen in bulk. The unit cell probed by STM reveals exactly the $p(1 \times 1)$ unit cell as

terminated from the bulk orthorhombic structure [or the $(\sqrt{2} \times \sqrt{2})R45^{\circ}$ one from the termination of a tetragonal structure]. The current image shown in Fig. 2(c), obtained simultaneously with the constant-current topographic image shown in Fig. 2(b), is a map of the tunneling current. While the topographic image in Fig. 2(b) was taken in the constant-current mode, the image in Fig. 2(c) reflects a very fine feedback signal as the tip is scanned along the surface. This current image is known to remove the large corrugation of features and reveals details that would otherwise be overwhelmed by the large background features. Figure 2(c) shows that the dark features in Fig. 2(b) are not caused by the missing atoms of the lattice, but occur because of the slightly lower integrated DOS in these areas. These features have been confirmed repeatedly on all the $BaFe_2As_2$ samples we have studied.

Figure 2(d) shows a tunneling spectrum taken at 4.3 K on the flat area with a $p(1 \times 1)$ lattice and absence of either adatoms or defects. This spectrum is representative of all locations as long as the tip is not located on top of or close to the bright scattered atoms. Even on top of the dislocations and in those dark features as appearing in Fig. 2(b), the tunneling spectra still preserve the same line shape, with slightly lower total intensities. The spectrum is asymmetric about the Fermi energy ($V = 0$). However, there are noticeable DOS features at -55 and $+45$ mV [indicated by arrows in Fig. 2(d)], while their origins are yet to be identified.

From the crystal structure point of view, there are only two possibilities for cleavage: one is between the Ba and As planes (see Fig. 1), and the other is between the As and Fe planes. The latter is very unlikely because of the strong bonding between the As and Fe. In the former case, some differences between the two different surfaces are expected to be seen—the As termination and the Ba termination (Fig. 1), which is also never observed. After experiments on many crystal samples, we are convinced that the cleaved surface of $BaFe_2As_2$ is As terminated and the Ba layer in the bulk is destroyed by cleaving. The random coverage of the scattered and clustered atoms that are seen in the STM images (white dots) are the Ba atoms remaining on the surface after cleaving. Obviously, the Ba atoms do not maintain their original lattice structure nor do they form any new superstructure. The observed squarelike lattice is the As terminated $p(1 \times 1)$ surface of the low-T orthorhombic phase [see Fig. 1(b)]. There is no evidence for surface reconstruction.

For a quantitative determination of surface termination and structure, LEED $I(V_i)$ was used. Because of its low Debye temperature [14] the sample was cooled to low T for good quality LEED $I(V_i)$ data collection. The LEED image taken at 20 K using a beam energy of 122 eV is shown in Fig. 3(a). The unit cell derived from the LEED pattern appears to reflect a (1×1) surface for a tetragonal structure, rather than a surface for an orthorhombic structure, as observed by STM. The beams that appear only in the orthorhombic phase seem to be missing, such as the (1,0) beam [expected at the position indicated by the arrow in Fig. 3(a)]. The question is: are they completely missing or just weak, hiding in the intense diffuse background originating from the random Ba adatoms on the surface?

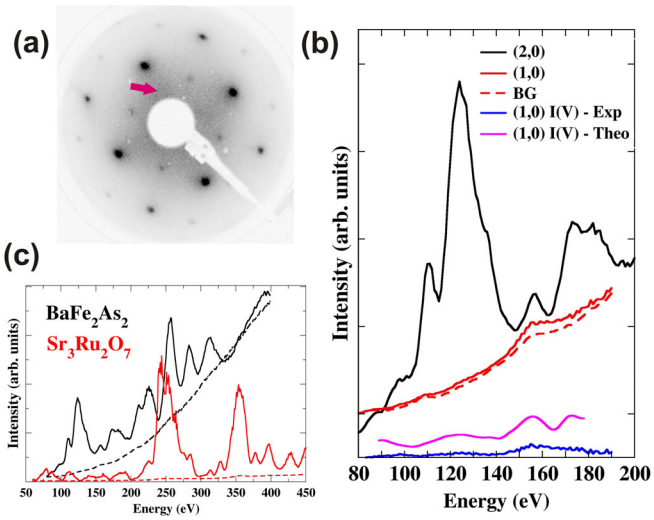

FIG. 3 (color online). (a) LEED image for the $BaFe_2As_2(001)$ surface obtained for an energy of 122 eV and at a temperature of 20 K. (b) Comparison between experimental $I(V_i)$ curves for the (1,0) and (2,0) without background (BG) subtraction. The dashed line represents the background for (1,0). The bottom curves are the theoretical and experimental $I(V_i)$ curves for (1,0). The theoretical intensities have been scaled for better visualization. (c) Comparison between typical experimental $I(V_i)$ curves of (2,0) beams for the $BaFe_2As_2$ and $Sr_3Ru_2O_7$ orthorhombic systems, with corresponding backgrounds (dashed lines).

The advantage of our data collection procedure is that all the data are stored, allowing us to analyze carefully the intensities as a function of energy for any parallel momentum ($k_{\|}$), as well as the energy-dependent background. The black curve in Fig. 3(b) is the intensity as a function of beam energy for $k_{\|} = (2, 0)$, a strong diffraction spot in Fig. 3(a). The red curve in Fig. 3(b) is the intensity for the orthorhombic $p(1 \times 1)$ $k_{\|} = (1, 0)$ direction. The energy dependence of the background is also presented. The blue curve at the bottom is the $k_{\|} = (1, 0)$ intensity with the background subtracted. As can be seen, the (1,0) beam is very weak, as expected from our calculations for the orthorhombic structure, but it is detectable with careful analysis, as shown in Fig. 3(b). The theoretical $I(V_i)$ curve for (1,0) is also presented for comparison. Some of the features (peaks) in (1,0) are in qualitative agreement with the calculations, but the poor signal-to-noise ratio and limited energy range of this beam do not make it useful for determining the details of the surface structure. The low intensity of the beams associated with the orthorhombic structure can be attributed to two facts: (i) the displacement of the Fe atoms due to orthorhombic distortions is in-plane and very small (~0.015 Å) [14,15], and (ii) LEED is primarily sensitive to the vertical displacement of the atoms.

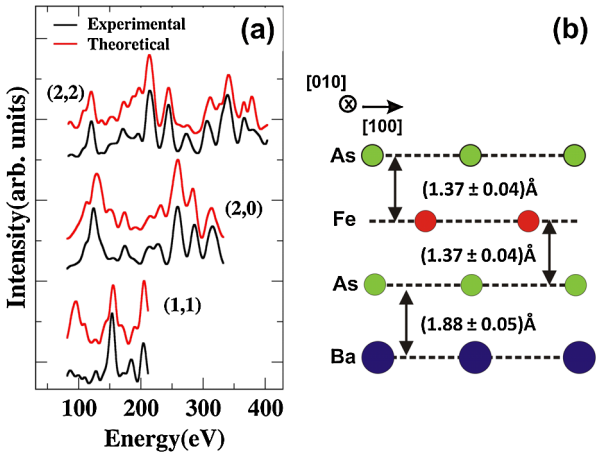

FIG. 4 (color online). (a) The measured $I(V_i)$ curves of the diffracted beams (1,1), (2,0), and (2,2) compared with the theoretical ones for the final As terminated surface structure. (b) The (001) surface structure obtained from LEED structural analysis. The bulk As-Fe and As-Ba interlayer distances are 1.3437 and 1.8926 Å, respectively [14].

In addition, the low Debye temperature of the constituting elements of $BaFe_2As_2$ also contribute to a small signal-to-background ratio. As can be seen in Fig. 3(c), there is an intense energy-dependent background associated with (2,0). For comparison, the intensity of a typical $I(V_i)$ curve (and background) for another orthorhombic system, $Sr_3Ru_2O_7(001)$ (our work), is also presented in Fig. 3(c). This bilayered perovskite is amenable to cleavage along (001), resulting in a well-ordered Sr-O terminated surface. The energy-dependent background for $Sr_3Ru_2O_7$ is much less intense, thus giving a higher signal-to-background ratio. The large background for $BaFe_2As_2(001)$ is a direct consequence of the Ba adatoms randomly scattered on the surface.

Given the fact that the surface has a structure with orthorhombic symmetry, quantitative structural analyses were performed by constraining the surface structure to a $p2mm$ symmetry (the 2D-symmetry representation of the $Fmmm$ orthorhombic symmetry). Nine symmetrically independent beams [(1,1), (2,0), (0,2), (2,2), (1,3), (3,1), (4,0), (0,4), and (3,3) in orthorhombic notation], measured at 20 K over a total energy range of 2155 eV, were used in the structural analyses. Shown in Fig. 4(a) are some of the $I(V_i)$ curves between 80 and 410 eV. The structural refinement has been performed through theoretical multiple scattering calculations described elsewhere [16], and the Pendry R factor (R_P) [17] was used to quantify the theory-experiment agreement.

Three different possible terminations for the $BaFe_2As_2(001)$ surface were investigated: (i) Ba termination; (ii) As termination; and (3) Fe termination in which the As-Fe-As trilayer is broken. The theory-experiment quantitative comparison demonstrates that the surface is As terminated, with $R_P = 0.24$ compared with 0.57 for Ba termination and 0.45 for Fe termination. The R_P value obtained for the As terminated surface, (0.24 ± 0.03), indicates a very good theory-experiment agreement for such a complex system. The obtained results, as presented in Fig. 4(b) for the As terminated model, confirm that the surface structure is basically orthorhombic bulk-truncated. The only difference is that the refined thickness (2×1.37 Å) of the As-Fe-As trilayer is slightly larger than that (2×1.34 Å) in the bulk, suggesting a possible small surface relaxation, but no reconstruction. The calculated beams of (1,1), (2,0), and (2,2) for the final As terminated surface structure are displayed in Fig. 4(a) to show the agreement with measured experimental results.

This work, combining real-space imagining and momentum-space diffraction, has shown that the cleaved surface of the $BaFe_2As_2$ single crystals is an ordered As terminated layer, with disordered Ba adatoms. Quantitative analyses indicate that the surface structure represents the low-temperature orthorhombic phase in bulk, without surface reconstruction. Importantly, our STM images reveal a different Fe-As orbital structure associated with the two distinct As atoms in the surface orthorhombic unit cell. Occasionally the STM images reveal a striped (1×2) configuration, which dominates images of doped superconducting phase [13]. It is possible that the (1×2) striped regions are stabilized by defects, vacancies, interstitial atoms, impurities, or dopants.

This effort was supported in part by the Division of Materials Science and Engineering, Basic Energy Sciences, U.S. DOE (A. S., M. A. M., B. C. S., D. M.). X. B. H., G. L., T. Y. C., and E. W. P. have received support from NSF and DOE (DMS&E and NSF-DMR-0451163). J. Z. is supported by NSF under grant No. DMR-0346826. This work is also partly supported by the State of Texas through TcSUH and the Robert A. Welch Foundation. We would also like to thank DMSE and Division of User Facilities for work at CNMS.

*vnascimento@lsu.edu

[1] Y. Kamihara *et al.*, J. Am. Chem. Soc. **128**, 10 012 (2006).
[2] Y. Kamihara *et al.*, J. Am. Chem. Soc. **130**, 3296 (2008).
[3] H. Ogino *et al.*, arXiv:0903.3314.
[4] Q. Huang *et al.*, Phys. Rev. B **78**, 054529 (2008).
[5] M. A. McGuire *et al.*, Phys. Rev. B **78**, 094517 (2008).
[6] Guodong Liu *et al.*, arXiv:0904.0677v2.
[7] G. F. Chen *et al.*, Phys. Rev. Lett. **100**, 247002 (2008).
[8] J. Dong *et al.*, Europhys. Lett. **83**, 27006 (2008).
[9] J. T. Park *et al.*, Phys. Rev. Lett. **102**, 117006 (2009).
[10] J. S. Kim *et al.*, J. Phys. Condens. Matter **21**, 102203 (2009).
[11] R. G. Moore *et al.*, Phys. Rev. Lett. **100**, 066102 (2008).
[12] R. Matzdorf *et al.*, Science **289**, 746 (2000).
[13] Yi Yin *et al.*, Physica (Amsterdam) **469C**, 535 (2009).
[14] M. Rotter *et al.*, Phys. Rev. B **78**, 020503(R) (2008).
[15] A. S. Sefat *et al.*, Phys. Rev. Lett. **101**, 117004 (2008).
[16] V. B. Nascimento *et al.*, Phys. Rev. B **75**, 035408 (2007).
[17] J. B. Pendry, J. Phys. C **13**, 937 (1980).